LETTERS

The presence of methane in the atmosphere of an extrasolar planet

Mark R. Swain[1]*, Gautam Vasisht[1]* & Giovanna Tinetti[2]*

Molecules present in the atmospheres of extrasolar planets are expected to influence strongly the balance of atmospheric radiation, to trace dynamical and chemical processes, and to indicate the presence of disequilibrium effects. As molecules have the potential to reveal atmospheric conditions and chemistry, searching for them is a high priority. The rotational–vibrational transition bands of water, carbon monoxide and methane are anticipated to be the primary sources of non-continuum opacity in hot-Jupiter planets[1–3]. As these bands can overlap in wavelength, and the corresponding signatures from them are weak, decisive identification requires precision infrared spectroscopy. Here we report a near-infrared transmission spectrum of the planet HD 189733b that shows the presence of methane. Additionally, a resolved water vapour band at 1.9 μm confirms the recent claim[4] of water in this object. On thermochemical grounds, carbon monoxide is expected to be abundant in the upper atmosphere of hot-Jupiter planets, but is not identifiable here; therefore the detection of methane rather than carbon monoxide in such a hot planet[5,6] could signal the presence of a horizontal chemical gradient away from the permanent dayside, or it may imply an ill-understood photochemical mechanism that leads to an enhancement of methane.

To date, molecular signatures have not been resolved in the emission spectra of hot-Jupiter extrasolar planets[7–10] (exoplanets). Transmission spectroscopy during the primary eclipse (when the planet occults a portion of the stellar disk, and a fraction of light from the star is seen after traversal through the atmosphere around the planet's limb) has the advantage of being insensitive to temperature structure in the exoplanet's atmosphere[11]. Owing to the presence of strong molecular absorption bands, near-infrared spectroscopy from 1 to 2.5 μm is well suited for detection of the signatures of H_2O, CO and CH_4. For a hot-Jupiter atmosphere in purely thermochemical equilibrium, the dominant carbon-bearing molecule is expected to be CO at higher temperatures (temperature $T > 1{,}200$ K) and CH_4 at lower temperatures ($T < 800$ K). On the daysides of the short-period, tidally locked hot-Jupiters, the local carbon chemistry should be dominated by CO; disequilibrium effects may result in CO as the dominant carbon-carrying molecule, even on the terminators and nightsides of such planets[6]. Our detection of the onset of the CH_4 bandhead at 2.2 μm is the first clear spectral signature of a carbon-based molecule in an exoplanet atmosphere.

We observed the transiting exoplanet HD 189733b with the Hubble Space Telescope using the NICMOS (NIC-3) camera on 25 May 2007, over five contiguous spacecraft orbits. During these observations, NICMOS was configured to obtain a spectrophotometric time series between 1.4 and 2.5 μm. As the parent star, HD 189733, is extremely bright (K-band magnitude $K = 5.52$), we defocused the NICMOS camera to increase the saturation time of individual detector pixels. This provided additional benefits for precision photometry[12] by allowing some spatial averaging over intra-pixel and pixel-to-pixel quantum efficiency variations that could couple to rapid telescope pointing errors and slow pointing drifts to produce spurious intensity fluctuations in the measured time series. The defocus determines the spectral resolution, allowing us to extract 18 independent wavelength channels with sufficient signal-to-noise ratio. There are gaps in the measured time series because the star HD 189733 is not in the 'continuous viewing zone' of the spacecraft, and, because of scheduling constraints, the in-eclipse data are not symmetric about the epoch of inferior conjunction.

During primary eclipse, the apparent brightness of the star decreased by ~2.4% (Fig. 1). However, as the modulation amplitude due to nominal amounts of water vapour[13] is predicted to be small (<0.1%), high-dynamic-range (~10^4) spectra are required to detect and characterize any molecular features. Although the Hubble Space Telescope avoids the limitations imposed by the Earth's atmosphere, spectrophotometry with NICMOS or other on-board instruments[12,14] is subject to systematic errors that must be corrected

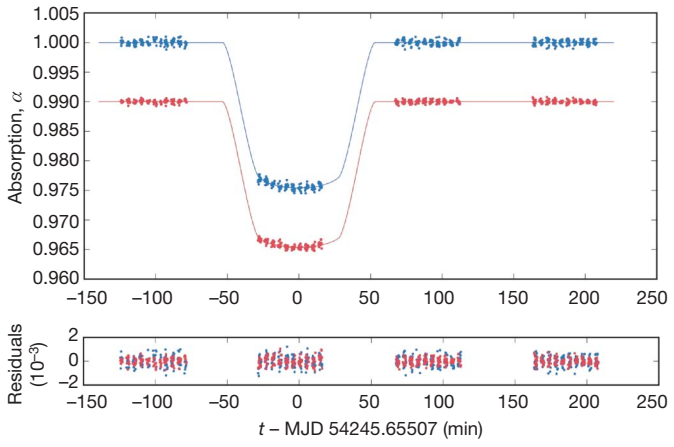

Figure 1 | Calibrated measurements showing the primary eclipse event. Top panel, the measured time series (where α is the percent absorption and t is time in units of minutes of modified Julian day, MJD), corrected for systematic errors, taken during four orbits of the Hubble Space Telescope. The primary eclipse occurs during the second orbit, and the curvature of the eclipse light curve is due to limb darkening of the star. The two time series shown are co-added spectral data approximately matching the H and K astronomical bands (blue, 1.6–1.8 μm; red, 2.0–2.4 μm). The gaps in the time series are because HD 189733 is not in the continuous viewing zone for the Hubble Space Telescope. For clarity, the red light curve has been offset. Bottom panel, residuals that correspond to the difference between the measured light curve and the model.

[1]Jet Propulsion Laboratory, California Institute of Technology, 4800 Oak Grove Drive, Pasadena, California 91109-8099, USA. [2]Department of Physics and Astronomy, University College London, Gower Street, London WC1E 6BT, UK.
*These authors contributed equally to this work.

©2008 Nature Publishing Group

because the errors are similar in size to the expected molecular signatures. In our data, the first orbit had strong systematic offsets (due to spacecraft settling) and was excluded from our analysis.

In order to arrive at the transmission spectrum, it is important to establish a proper baseline for the remaining out-of-eclipse data. The systematic errors in the raw light curves are dominated by two types, correlations in time and in wavelength. In order to remove temporal correlations, we assumed that the observed flux in each wavelength channel for the out-of-eclipse orbits could be modelled by perturbations that were linear in five state variables, and by a term that was up to parabolic in spacecraft orbital phase. The state variables capture the optical state of the camera and are the centroids of channels, a variable defocus due to 'breathing' of the telescope focus, rotation of the spectrum with respect to the detector, and temperature. A regression to the observed light curves provided the coefficients of the model. When decorrelated on the basis of the model, the time series showed no further temporal correlations. Some remaining excess noise was strongly correlated in wavelength; an estimator for this noise was constructed as a weighted average of all channel time series data (collapsed in the wavelength axis) and was then subtracted from individual channels. The resulting channel time series are near the theoretical noise limit. The robustness of the fits was verified by removing sections of the data from the fit and ensuring that the combined residuals remain well behaved.

The in-eclipse time series temporal effects were decorrelated by applying the model coefficients determined from the out-of-eclipse data to state variables and the spacecraft orbital phase at every time-step during that orbit. After accounting for the chromatic effects introduced in the eclipse light curve by limb darkening, a wavelength decorrelation was performed using the same method as was used for the out-of-eclipse orbits. The transit time series, now also corrected for instrument systematics, was averaged to construct a transmission spectrum. This spectrum includes astrophysical biases that have weak chromatic dependence, due to averaging over limb-darkened light curves and also due to the presence of cool starspots on the disk of the star. The effect of limb darkening, though not as dramatic as in optical data, is clearly seen as curvature in the eclipse light curves (Fig. 1). We co-added the spectral channels to construct synthetic light curves matching the H and K astronomical bands, for which there are published nonlinear, limb-darkening laws[15]. We then constructed a computer model of a limb-darkened star, and simulated the motion of the planet across the stellar disk using the system's keplerian parameters[14,16] to generate model light curves. A steepest descent scheme was used to fit generated curves to the measured data by leaving the planet effective radius (in that band) and epoch of transit as free parameters. The best-fit light curves in each band were used to estimate the limb-darkening biases; the mean correction is 2×10^{-4}, and the colour correction is 1×10^{-4} across the band. The presence of starspots on HD 189733 has been inferred[16] from measurements of long-term, out-of-eclipse variability, and from the structure of transit light curves at optical wavelengths[14]. Unocculted starspots introduce a positive chromatic bias in the inferred absorption depth, as they are cooler than the stellar disk; in the infrared, the chromaticity of this effect is small and monotonic, and thus has little effect on the shape of the observed modulation. We derived a correction with a starspot coverage of 4% using model spectra[17] and assuming that the starspots were on average 1,000 K cooler than the 5,000 K stellar photosphere. A more detailed description of the data reduction method is available (Supplementary Information).

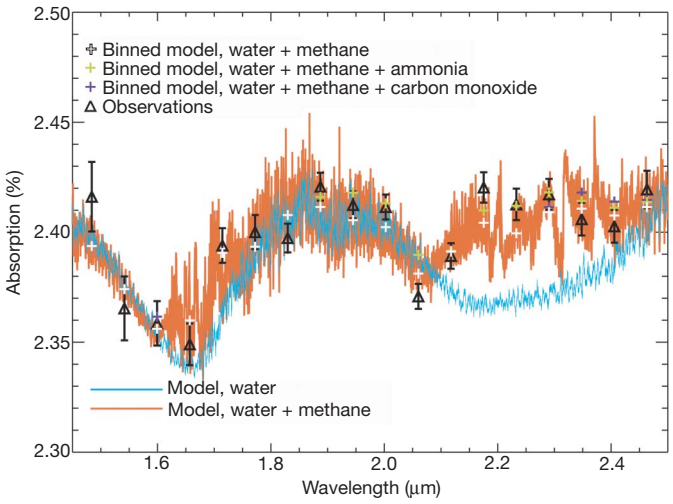

Figure 2 | A comparison of observations with simulated water and methane absorption. The measured spectrum (black triangles), and two theoretical spectra of the predominantly H_2 atmosphere, showing the effects of small amounts of water (blue) and methane in combination with water (orange). The measured spectrum contains significant differences at 1.7–1.8 μm and at 2.15–2.4 μm from what is expected due to water vapour alone. We interpret these departures as additional absorption features due to the presence of one or more other species in addition to water. When considering only water and methane, the theoretical spectrum best fitting the data was determined by binning the model (shown as white crosses) to the spectral resolution of the observations. Different model predictions based on changing abundances and molecules were compared to the observations using the reduced χ^2; the best fitting model has a water abundance of 5×10^{-4} and a methane abundance of 5×10^{-5}. The model spectrum can be improved slightly with the addition of small ($\sim 1 \times 10^{-5}$) amounts of either ammonia or carbon monoxide (shown in green and purple crosses, respectively). Error bars show $\pm 1\sigma$; the error includes the uncertainty in the correction of systematic effects (see Supplementary Information). Note that determining the zero point for the spectrum depends on the diameter assumed for the planet and assumptions in the starspot correction. Thus, the shape of the spectrum is robust; there is an uncertainty of $\pm 2 \times 10^{-4}$ in the absolute level.

We show the corrected spectrum as relative absorption depth in Fig. 2. The signature of the H_2O absorption band centred around 1.9 μm is immediately obvious. The steep increase in absorption at the short-wavelength edge is also most probably due to an adjacent water band centred at a wavelength less than 1.5 μm. Thus, the new spectrum allows an unambiguous identification of water vapour in the atmosphere of HD 189733b, confirming its earlier inference from broadband photometry[4]. As a steep change in absorption occurs at 2.2 μm, the observations decisively show that methane is present in addition to water. To explore the abundance of H_2O and CH_4 and possible contributions of CO and NH_3, simulated transmission spectra were generated using a recent version of a planetary spectral model[13]. The model covers a range of pressure from ~ 10 to $\sim 10^{-10}$ bar and includes transitions[18] for H_2–H_2 (the most common molecular species). The temperature and density at each atmospheric level are determined by the pressure–temperature profile, and the absorption contribution from each molecule is computed on the basis of its mixing ratio. The H_2O absorption coefficients incorporate a new, high-accuracy line list[19], and the CO absorption coefficients were estimated with the HITEMP data base (L. S. Rothman *et al.*, personal communication). The CH_4 absorption coefficients were evaluated using a combination of line lists[20,21]. For all the molecules, the opacities are calculated for the selected spectral band at the different temperatures of the atmospheric layers (from 500 K to 2,000 K) and in some cases[18,21] interpolated for intermediate values of the available temperatures. We used the 'evening terminator' pressure–temperature profile[22]; significantly different temperature profiles produce results that do not match the observed water vapour absorption features. The theoretical spectra were binned to the same spectral resolution as the measurements, and the results of different compositions were compared with the observations using the reduced χ^2 value. Combinations of H_2O and CO, as well as H_2O and NH_3, failed to match the observed spectrum. The model best fitting the observations has a mixing ratio of $\sim 5 \times 10^{-4}$ for H_2O, and

©2008 Nature Publishing Group

5×10^{-5} for CH_4 (see Fig. 2); the addition of NH_3 with a mixing ratio of 1×10^{-5} improves the fit slightly. The agreement between our H_2O mixing ratio value and previous results[4] is significant because a wide range of wavelengths, covering three major H_2O absorption bands, can be modelled self-consistently; this implies that the estimated H_2O mixing ratio is robust. The pressure at which the atmosphere becomes optically thick ranges from a few millibars, when the absorption is strong, to ~0.2 bar, when the absorption is weaker (for example, ~1.7 μm). We have modelled the effect of aerosols and determined that our spectrum is haze-free, as their contribution would depress the spectral signature of both H_2O and CH_4 relative to the measured absorption depth. If aerosols are present, as is suggested by recent measurements[23], they must be in the form of small particles and their effects confined to wavelengths shorter than 1.5 μm (ref. 24).

Although we can unambiguously determine that CH_4 is present, the CH_4 abundance estimate is dependent on uncertainties in the high-temperature transitions. Additionally, the presence of CH_4 masks the effect of CO in the absorption spectrum. Although the best fit is obtained using only H_2O and CH_4, CO can be included up to the abundance of H_2O with a modest increase in χ^2. Thus, we cannot strongly constrain abundance of CO or the elemental C/O ratio. The relatively high concentration of CH_4 could be due in part to photochemistry. Photolysis of CO and CH_4 is probably not significant in the upper atmosphere (pressure $P < 10^{-4}$ bar) of HD 189733b because of the strength of C–O and C–H bonds and the deficit of ultraviolet flux from its cool parent star (spectral type K2V). However, the photolysis of the weaker bonds of sulphur-, nitrogen- and oxygen-bearing compounds and the accompanying availability of fast-reacting free radicals could have a significant effect on the relative abundance[25] of CH_4 compared to CO.

Received 14 September 2007; accepted 6 February 2008.

1. Seager, S. & Sasselov, D. D. Theoretical transmission spectra during extrasolar giant planet transits. *Astrophys. J.* **537,** L916–L921 (2000).
2. Burrows, A. A theoretical look at the direct detection of giant planets outside the Solar System. *Nature* **433,** 261–268 (2005).
3. Fortney, J. J., Cooper, C. S., Showman, A. P., Marley, M. S. & Freedman, R. S. The influence of atmospheric dynamics on the infrared spectra and light curves of hot Jupiters. *Astrophys. J.* **652,** 746–757 (2006).
4. Tinetti, G. *et al.* Water vapour in the atmosphere of a transiting extrasolar planet. *Nature* **448,** 169–171 (2007).
5. Knutson, H. A. *et al.* A map of the day–night contrast of the extrasolar planet HD 189733b. *Nature* **447,** 183–186 (2007).
6. Cooper, C. S. & Showman, P. Dynamics and disequilibrium carbon chemistry in hot Jupiter atmospheres with application to HD 209458b. *Astrophys. J.* **649,** 1048–1063 (2006).
7. Richardson, L. J., Deming, D., Horning, K., Seager, S. & Harrington, J. A spectrum of an extrasolar planet. *Nature* **445,** 892–895 (2007).
8. Grillmair, C. J. *et al.* A Spitzer spectrum of the extrasolar planet HD 189733b. *Astrophys. J.* **658,** L115–L118 (2007).
9. Swain, M. R., Bouwman, J., Akeson, R. L., Lawler, S. & Beichman, C. A. The mid-infrared spectrum of the transiting exoplanet HD 209458b. *Astrophys. J.* **674,** 482–498 (2008).
10. Fortney, J. J. & Marley, M. S. Analysis of Spitzer spectra of irradiated planets: Evidence for water vapor? *Astrophys. J.* **666,** L45–L48 (2007).
11. Hubbard, W. B. *et al.* Theory of extrasolar giant planet transits. *Astrophys. J.* **560,** 413–419 (2001).
12. Gilliland, R. L. & Arribas, S. High signal-to-noise differential NICMOS spectrophotometry. *Instrum. Sci. Rep. NICMOS* **2003-001,** 1–14 (2003).
13. Tinetti, G. *et al.* Infrared transmission spectra for extrasolar giant planets. *Astrophys. J.* **654,** L99–L102 (2007).
14. Pont, F. *et al.* Hubble Space Telescope time-series photometry of the planetary transit of HD189733: No moon, no rings, starspots. *Astron. Astrophys.* **476,** 1347–1355 (2007).
15. Claret, A. A new non-linear limb-darkening law for LTE stellar atmosphere models. Calculations for $-5.0 \leq \log[M/H] \leq +1$, $2000 \leq T_{eff} \leq 50000$ K at several surface gravities. *Astron. Astrophys.* **363,** 1081–1190 (2000).
16. Winn, J. N. *et al.* The transit light curve project V. System parameters and stellar rotation period of HD 189733. *Astron. J.* **133,** 1828–1835 (2007).
17. Hauschildt, P. H., Allard, F. & Baron, E. The NextGen model atmosphere grid for $3000 < T_{eff} < 10{,}000$ K. *Astrophys. J.* **512,** 377–385 (1999).
18. Borysow, A., Jorgensen, U. G. & Fu, Y. High temperature (1000–7000K) collision induced absorption of H_2 pairs computed from first principles, with application to cool and dense stellar atmospheres. *J. Quant. Spectrosc. Radiat. Transf.* **68,** 231–255 (2001).
19. Barber, R. J., Tennyson, J., Harris, G. J. & Tolchenov, R. A high accuracy computed water line list. *Mon. Not. R. Astron. Soc.* **368,** 1087–1094 (2006).
20. Rothman, L. S. *et al.* The HITRAN 2004 molecular spectroscopic database. *J. Quant. Spectrosc. Radiat. Transf.* **96,** 139–204 (2005).
21. Nassar, R. & Bernath, P. Hot methane spectra for astrophysical applications. *J. Quant. Spectrosc. Radiat. Transf.* **82,** 279–292 (2003).
22. Burrows, A., Sudarsky, D. & Hubeny, I. Theory for the secondary eclipse fluxes, spectra, atmospheres and light curves of transiting extrasolar giant planets. *Astrophys. J.* **650,** 1140–1149 (2006).
23. Pont, F., Knutson, H., Gilliland, R. L., Moutou, C. & Charbonneau, D. Detection of atmospheric haze on an extrasolar planet: The 0.55 – 1.05 micron transmission spectrum of HD189733b with the Hubble Space Telescope. *Mon. Not. R. Astron. Soc.* (in the press).
24. Brown, T. M. Transmission spectra as diagnostics of extrasolar giant planet atmospheres. *Astrophys. J.* **533,** 1006–1026 (2001).
25. Liang, M.-C., Seager, S., Parkinson, C. D., Lee, A. Y.-T. & Yung, Y. L. On the insignificance of photochemical hydrocarbon aerosols in the atmospheres of close-in extrasolar giant planets. *Astrophys. J.* **605,** L6–L64 (2004).

Supplementary Information is linked to the online version of the paper at www.nature.com/nature.

Acknowledgements We thank D. Deming for contributions to the original proposal and for suggestions for clarifying the material presented in the manuscript. We thank T. Wiklind, N. Pirzkal and other members of the Space Telescope Science Institute staff for assistance in planning the observations and for advising how the observations could be optimized. We also thank K. Jahnke for suggesting the long-wavelength NICMOS grism, F. Pont for discussions concerning the treatment of the data, M.-C. Liang for discussions on photolysis, and J. Tennyson and R. Barber for suggestions on the methane data lists. G.T. was supported by the UK Sciences & Technology Facilities Council and the European Space Agency. The research described in this paper was carried out at the Jet Propulsion Laboratory, California Institute of Technology, under a contract with NASA.

Author Contributions M.R.S. was the PI of the project and led the overall direction of the research. G.V. led the data analysis and G.T. led the modelling. All authors contributed equally to the writing of the paper.

Author Information Reprints and permissions information is available at www.nature.com/reprints. Correspondence and requests for materials should be addressed to M.R.S. (Mark.R.Swain@jpl.nasa.gov).

©2008 Nature Publishing Group